Hole distribution between the Ni 3*d* and O 2*p* orbitals in $Nd_{2-x}Sr_xNiO_{4-\delta}$

Z. Hu, M. S. Golden, and J. Fink
Institut für Festkörper- und Werkstofforschung Dresden, P.O. Box 270016, D-01171 Dresden, Germany

G. Kaindl
Institut für Experimentalphysik, Freie Universität Berlin, Arnimallee 14, D-14195 Berlin-Dahlem, Germany

S. A. Warda and D. Reinen
Fachbereich Chemie und Zentrum für Materialwissenschaften, Philipps-Universität Marburg, Lahnberge, D-35032 Marburg, Germany

Priya Mahadevan and D. D. Sarma
Solid State and Structural Chemistry Unit, Indian Institute of Science, Bangalore 560012, India

(Received 13 July 1999)

We present a joint experimental and theoretical study of x-ray absorption at the O-K and Ni-$L_{2,3}$ thresholds of $Nd_{2-x}Sr_xNiO_{4-\delta}$ providing an analysis of the distribution of doped holes induced by Sr substitution between Ni 3*d* and O 2*p* orbitals. The preedge peak in the O-K x-ray absorption (XAS) spectra, reflecting holes located in the O 2*p* orbitals, increases monotonically with the degree of Sr doping up to the maximum doping level studied ($x=1.4$). The saturation in the relative intensity of the O-K preedge peak in the analogous lanthanum nickelate reported in the literature is shown to be most likely due to surface oxygen deficiency. Furthermore, the experimental Ni-$L_{2,3}$ XAS spectrum of the Ni(III) nickelate $Nd_{1.1}Sr_{0.9}NiO_{3.95}$ was simulated by a cluster approach, including charge-transfer and complete multiplet interactions, and compared with the corresponding spectrum of the Ni(III) system $Nd_2Li_{0.5}Ni_{0.5}O_4$. The $3d^7$ weight in the ground state of $Nd_{1.1}Sr_{0.9}NiO_{3.95}$ was found to be 42%, somewhat smaller than the value of 51% found for $Nd_2Li_{0.5}Ni_{0.5}O_4$. This indicates the influence of nonlocal effects in x-ray-absorption spectroscopy, which, in this case is due to the increased covalency in the Sr-doped system as a result of inter-NiO_6-cluster interaction. Such interactions are absent in $Nd_2Li_{0.5}Ni_{0.5}O_4$, which is characterized by having isolated NiO_6 clusters.

I. INTRODUCTION

The electronic and magnetic properties of the nickelate $La_{2-x}Sr_xNiO_{4-\delta}$ have been extensively studied in the past[1–4] as it possesses many features similar to those of the high-T_c superconductor $La_{2-x}Sr_xCuO_{4-\delta}$. Both systems have the same basic tetragonal K_2NiF_4 structure, which consists of an alternate stacking of KF rock-salt-type layers and $KNiF_3$ perovskite-type layers.[5] Their parent compounds La_2NiO_4 and La_2CuO_4 possess antiferromagnetic order that disappears at low doping levels.[6] There are, however, some striking differences between the two systems. $La_{2-x}Sr_xCuO_{4-\delta}$ turns metallic for $x>0.05$ and exhibits superconductivity for $0.05<x<0.3$. In contrast, $La_{2-x}Sr_xNiO_{4-\delta}$ becomes metallic only at much higher Sr doping levels ($x>1.0$) and does not turn superconducting. In the nickelate, for high doping levels, the NiO_6 octahedra are nearly equiaxial. Therefore the e_g orbitals are almost degenerate and the charge carriers are found in hybrid states that arise from interactions between the Ni$3d_{x^2-y^2}$/Ni$3d_{3z^2-r^2}$ states and the O 2*p* states. It has been suggested that strong electron-phonon coupling may well be the main reason for the insulating behavior of the doped ($x<1$) nickelates,[7,8] and the doped states have been discussed in terms of polarons which behave quantum mechanically on the length scale of the lattice constant.[7] For particular doping levels (e.g., $La_{1.5}Sr_{0.5}NiO_4$) polaron lattices or stripe phases have been observed in the doped nickelates.[9]

Regarding the nature of the doped charge carriers, it has generally been stated that the doped holes have mainly O 2*p* character in $La_{2-x}Sr_xNiO_{4-\delta}$,[7–11] in analogy to the situation in $La_{2-x}Sr_xCuO_{4-\delta}$.[12] For the nickelates this conclusion was based upon the observation of a pre-edge peak in the O-K x-ray-absorption (XAS) spectra whose intensity increases with increasing Sr doping. Up to now, however, studies by high-energy spectroscopies have been reluctant in discussing the issue of the number of holes located in Ni 3*d* states. This is a consequence of the overlap between the La-M_4 and the Ni-L_3 absorption thresholds, which prevents a thorough experimental and theoretical analysis of the Ni-$L_{2,3}$ XAS spectra.

In the present work we present the results of a joint experimental and theoretical study of the O-K and Ni-$L_{2,3}$ XAS spectra of the $Nd_{2-x}Sr_xNiO_{4-\delta}$ system, with particular emphasis put on high Sr doping levels. With the reasonable assumption that the identity of the trivalent lanthanide element in the block layers is not crucial for the electronic states in the NiO_2 plane, the choice of Nd instead of La brings the advantage of full accessibility of the Ni-$L_{2,3}$ absorption thresholds, thus enabling a study of the *distribution* of holes between O 2*p* and Ni 3*d* states.

In general, the $L_{2,3}$-XAS spectra of 3*d*-TM compounds have been reproduced successfully in the framework of charge-transfer multiplet calculations truncating the basis to retain only terms involving d^n and $d^{n+1}\underline{L}$ in the ground state as well as d^{n+1} and $d^{n+1}\underline{L}$ in the final state.[13] However, many-body interactions induced by covalency are important

for both Cu(III) and Ni(III) oxides.[14] In such situations, it has been shown recently that an approximation involving a truncated basis could result in erroneous parameters for strongly covalent compounds.[15] Thus in the calculations presented here we include the complete basis along with all the interaction terms (i.e., full multiplet, charge-transfer, and hopping interactions).

II. EXPERIMENTAL DETAILS

Solid samples of $Nd_{2-x}Sr_xNi_2O_{4-\delta}$ were prepared as described in Ref. 16 for the analogous La mixed crystals. The phase purity (>98%) was controlled by x-ray diffraction and the oxygen content was determined by iodometric titration. We will report about the phase characterization and further spectroscopic properties in detail elsewhere. The XAS measurements were performed at the SX700/II plane-grating-monochromator beamline operated by the Freie Universität Berlin at the Berliner Elektronenspeicherring für Synchrotronstrahlung (BESSY). For the O-K spectra, the fluorescence-yield (FY) mode with an escape depth of typically 2000 Å was used, while the Ni-$L_{2,3}$ data were taken in the total-electron-yield (TY) mode with a typical escape depth of 50 Å. The O-K spectra were corrected for the energy-dependent incident flux and for self-absorption effects according to a procedure described elsewhere,[17,18] and they were normalized at 60 eV above threshold. The experimental energy resolution was set to 0.3 and 0.6 eV at the O-K and Ni-L_3 thresholds, respectively. The surfaces of the samples were cleaned in UHV by scraping with a diamond file. Unfortunately, the surfaces of these highly oxidized TM compounds are not very stable in vacuum, particularly when exposed to x rays, leading to an oxygen deficiency in the surface layer. However, this is not a serious problem for the O-K XAS spectra recorded in the volume-sensitive FY mode. In order to limit the influence of such surface effects on the Ni-$L_{2,3}$ XAS spectra, the data acquisition time was restricted to ten minutes after each cleaning procedure. Under these conditions, the O-K and Ni-$L_{2,3}$ spectra of different samples with the same doping level measured during different beam times were found to be identical.

III. RESULTS AND DISCUSSION

A. O-K XAS spectra

To start with, and also to enable a detailed comparison with previous investigations, we discuss first the O-K XAS spectra of $Nd_{2-x}Sr_xNiO_{4-\delta}$ which are shown in Fig. 1 together with the spectrum of NiO as a reference. The observed spectral profiles of the Nd nickelates studied here are very similar to the previously published spectra of polycrystalline $La_{2-x}Sr_xNiO_4$ samples recorded in the TY mode, with x values up to 1.1,[8] as well as to data from single-crystalline samples recorded in the FY mode for x up to 0.6.[7] The main change in the spectral features with increasing doping level is an increase in the intensity and a shift to lower energy of the pre-edge peak below 530 eV, which is assigned to ligand hole states induced by doping. Polarization dependent XAS studies of single crystals[7] indicate that this peak is comprised of three features, related to final states with $^3B_1$, $^1A_1$, and $^1B_1$ symmetry (listed in order of increasing energy). These final states contain[7] either single holes in: the Ni $3d_{x^2-y^2}$ and $3d_{3z^2-r^2}$ orbitals in a high spin arrangement ($^3B_1$), the Ni $3d_{x^2-y^2}$ and $3d_{3z^2-r^2}$ orbitals in a low spin arrangement ($^1B_1$), or two holes in the Ni $3d_{x^2-y^2}$ orbital ($^1A_1$).

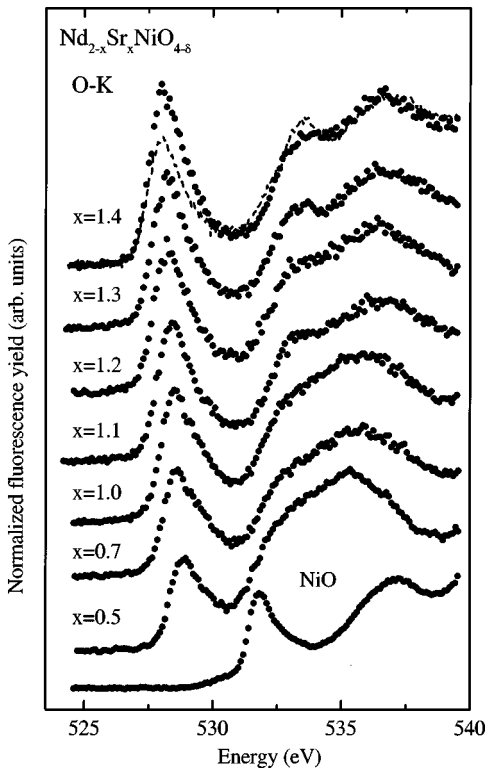

FIG. 1. O-K XAS spectra of $Nd_{2-x}Sr_xNiO_{4-\delta}$ together with that of NiO as reference. The data were recorded using the bulk-sensitive FY method (filled circles). For comparison, the spectrum obtained for the $x=1.4$ sample in the TY mode (dashed curve) is also given by the solid line. The solid curves through the data points serve as a guide to the eyes.

The feature at 531.8 eV in NiO, which is assigned to O $2p$ states hybridized with the Ni $3d$ related upper Hubbard band (UHB), is more or less absent in the spectra of the doped nickelates. This dynamic transfer of spectral weight from the UHB to the doping-induced state is an important characteristic of charge-transfer insulators.[12,19]

As regards the O-K edge data, the main difference with the previous observations for $La_{2-x}Sr_xNiO_{4-\delta}$ is that here the intensity of the pre-edge peak steadily increases with the Sr content, right up to the highest doping level of 1.4. In the data from the La system, the pre-edge peak decreased in intensity from $x=0.8$ to $x=1.1$.[8] This difference might be due to oxygen deficiency in the surface layer of the sample, which is a serious problem for higher Sr doping levels. In this context, we note that the TY mode used in Ref. 8 is significantly more sensitive to such surface oxygen deficiency than the FY mode employed here. To illustrate this, we also show the TY spectrum of the $x=1.4$ sample in Fig. 1 (dashed line), in addition to the data recorded in the FY mode. Our TY curve is similar to previously published data for the La system with $x=1.4$.[20] The lower spectral weight of the pre-edge peak in the TY spectrum in comparison with the FY spectrum reflects a lower concentration of oxygen hole states in the sample surface. The XAS data measured in the FY mode from single crystals,[7] with surfaces prepared *ex situ*, revealed a slowing down in the growth of the ligand-hole peak approaching the maximum doping level studied

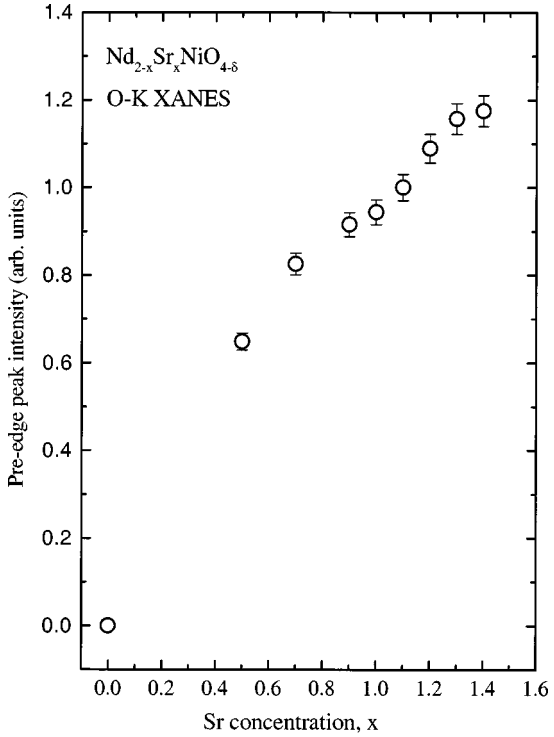

FIG. 2. Normalized intensity of the pre-edge peak in the O-K XAS spectra of $Nd_{2-x}Sr_xNiO_4$ as a function of doping (see text for details).

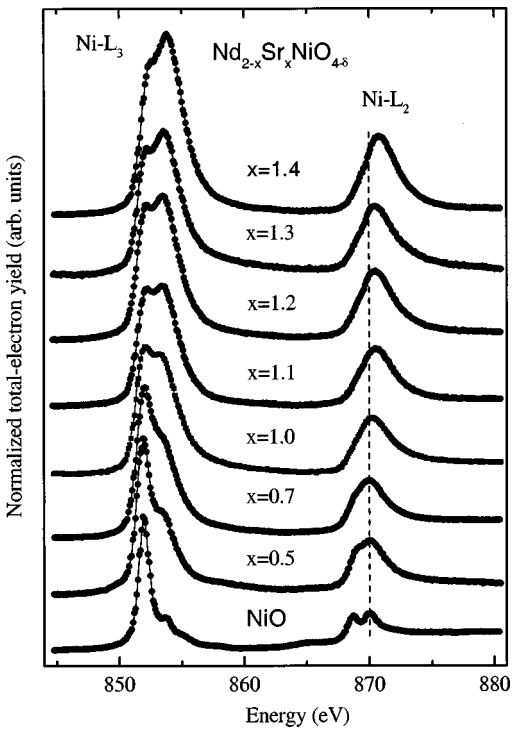

FIG. 3. Ni-$L_{2,3}$ XAS spectra of $Nd_{2-x}Sr_xNiO_4$ together with data from NiO as reference. The data were recorded using the TY method. The solid curves through the data points serve as a guide to the eyes.

($x=0.6$). For the data presented here, the evolution of the spectral weight (integrated areas) of the pre-edge peak with doping is summarized in Fig. 2. It is clear from this figure that the intensity grows with x up to $x=1.4$.

B. *Ni-$L_{2,3}$* XAS spectra

In this section, we first present the Ni-$L_{2,3}$ XAS spectra of the $Nd_{2-x}Sr_xNiO_{4-\delta}$ system, followed by a comparison of the two formal Ni(III) systems, $Nd_{0.9}Sr_{1.1}NiO_{3.95}$ and $Nd_2Li_{0.5}Ni_{0.5}O_4$. We will then discuss the physical picture used for an interpretation of such TM-$L_{2,3}$ XAS spectra, before proceeding on to the final section that deals with the results of the charge-transfer atomic-multiplet calculations.

1. *The Ni-$L_{2,3}$ XAS spectra of $Nd_{2-x}Sr_xNiO_{4-\delta}$*

Figure 3 shows the XAS spectra at the Ni-$L_{2,3}$ thresholds together with a spectrum of NiO for reference. We would like to point out that these are the first Ni-L_3 XAS data of the Sr-doped Lr_2NiO_4 system, which are free of overlap with spectral structures from other elements, i.e., these spectra show directly the experimental data and are not obtained by subtraction or other data manipulation procedures.

A striking change in the Ni-L_3 spectral structure is observed upon increasing the level of Sr doping. In particular, the spectral weight of the high-energy component at 853 eV (about 1.7 eV above the main peak in the Ni-L_3 XAS spectrum of NiO) increases dramatically with x, becoming the dominant feature for $x>1.0$. At the Ni-L_2 threshold, the lower energy component of the double-peaked structure loses intensity relative to the higher energy structure. This higher energy structure also shifts up in energy by about 0.5 eV for $x=1.4$. It is furthermore evident that the $L_{2,3}$ spectra as a whole turn progressively broader with increasing doping level. This broadening appears to be intrinsic to $Ln_{2-x}Sr_xNiO_{4-\delta}$ systems, in which the NiO_6 octahedra form an extended network. The spectrum of the $x=1.1$ material shown here [$\delta=0.05$, corresponding formally to Ni(III)] is qualitatively similar to that observed in a XAS study of $NdNiO_3$, performed with a somewhat better energy resolution.[21]

2. *Comparison of the two Ni(III) systems $Nd_{0.9}Sr_{1.1}NiO_{3.95}$ and $Nd_2Li_{0.5}Ni_{0.5}O_4$*

We now compare the two formally trivalent Ni systems, $Nd_{0.9}Sr_{1.1}NiO_{3.95}$ and $Nd_2Li_{0.5}Ni_{0.5}O_4$. Both of these materials crystallize in the K_2NiF_4 structure and contain low-spin Ni(III). The difference between these two compounds is the nature of the connection between the NiO_6 octahedra. In the former compound, the octahedra are linked via corner sharing to form two-dimensional planes. In the latter, the Li ions occupy every second Ni site in the plane, thus resulting in isolated NiO_6 octahedra.[16,22] A comparison of these two materials will therefore allow us to assess the impact of additional delocalization effects that arise from the interaction between neighboring NiO_6 clusters.

Figure 4 shows a comparison of the O-K and Ni-$L_{2,3}$ XAS spectra of the two compounds. The pre-edge peak in the O-K spectrum of $Nd_2Li_{0.5}Ni_{0.5}O_4$, presented in the left panel of Fig. 4, is shifted by 0.5 eV to higher energy relative to that of $Nd_{0.9}Sr_{1.1}NiO_{3.95}$ and is also narrower by 0.6 eV. A similar shift has been observed between the O-K absorption spectra of $Li_{1-x}Ni_xO$ and $La_{2-x}Sr_xNiO_4$ and was attributed

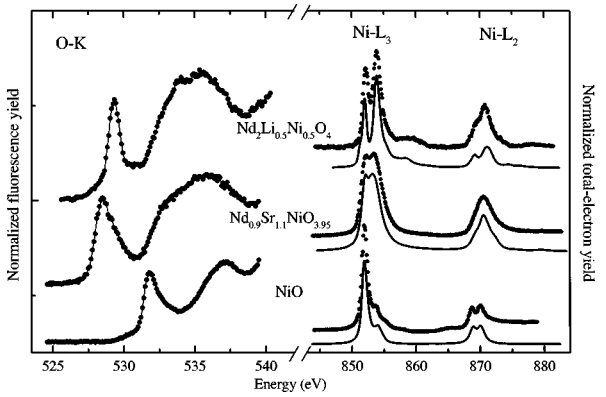

FIG. 4. O-K XAS (left panel) and Ni-$L_{2,3}$ XAS (right panel) spectra of the two formally trivalent Ni oxides, $Nd_{0.9}Sr_{1.1}NiO_{3.95}$ and $Nd_2Li_{0.5}Ni_{0.5}O_4$, together with NiO as reference. In the right panel, the solid curves below the data points are the results of charge-transfer atomic-multiplet calculations as described in the text.

to the different impurity potentials of the Li and Sr ions.[23] This point alone, however, is not enough to explain the similarity of the O-K XAS spectra of $La_{2-x}Sr_xNiO_{4+\delta}$ doped either by Sr ($\delta=0$, $x>0$) or by oxygen excess ($x=0$, $\delta>0$).[7,24] The crucial additional factor is the *site* within the structure at which the induction of doping takes place. A substitution at the Ni sites (Li in $Li_{1-x}Ni_xO$ or $Nd_2Li_{0.5}Ni_{0.5}O_4$) does not necessarily have the same effect as a substitution at sites in the block layers (Sr or excess O in $La_{2-x}Sr_xNiO_{4+\delta}$). Indeed, the isolation of the Ni sites caused by Li doping in $Nd_2Li_{0.5}Ni_{0.5}O_4$ leads to a narrow O-K pre-edge peak in this system;[14] it is therefore a manifestation of the localized nature of these doping-induced states. A similar conclusion concerning the nature of doped hole states was reached for the closely related system $La_2Li_{0.5}Cu_{0.5}O_4$ by recent local-density approximation (LDA)$+U_{dd}$ calculations.[25]

The Ni-$L_{2,3}$ XAS spectrum of $Nd_{0.9}Sr_{1.1}NiO_{3.95}$, shown in the right panel of Fig. 4, contains also significantly broader spectral features than that of $Nd_2Li_{0.5}Ni_{0.5}O_4$, and the weak satellite observed at about 6 eV above the higher energy component of the main peak in the latter spectrum is absent in the Sr-doped material. A similar satellite had been observed before in TM-$L_{2,3}$ XAS spectra of $NaCuO_2$ (Refs. 26 and 27) and $La_2Li_{0.2}Cu_{0.5}O_4$.[14] In the case of these cuprates, the satellite can be assigned to final states dominated by the $\underline{2p}3d^9$ configuration ($\underline{2p}$ denotes a hole in the $2p$ state).

3. Physical basis for the interpretation of the Ni-$L_{2,3}$ XAS spectra

In order to assess the charge distribution between the O and the TM sites in such hybridized systems, it is vital to consider not only the O-K XAS spectra but also to carry out a quantitative analysis of the TM-$L_{2,3}$ XAS data.[14] It is instructive at this stage to consider a simplified model for illustrating the essential ideas involved in the more complete treatment of the XAS spectra, which will be presented further below.

The Hamiltonian matrix and the ground state of a $3d^n$ system are given by (for simplicity we neglect any admixture of $d^{n+m}\underline{L}^m$ configurations with $m\geq 2$):

$$H=\begin{vmatrix} 0 & T \\ T & \Delta \end{vmatrix}, \tag{1}$$

$$\Phi_g=\alpha_0|3d^n\rangle+\beta_0|3d^{n+1}\underline{L}\rangle, \quad (\alpha_0^2+\beta_0^2)=1, \tag{2}$$

where Δ is the charge-transfer energy for the many-electron system; $\underline{L}$ denotes a hole in an O $2p$ orbital and T is the transfer integral between the TM $3d$ states and the ligand orbitals; Φ_g denotes the ground-state wave function of the system. The configuration mixing coefficients in the ground state, α_0 and β_0, are related to each other by the following equation:

$$\beta_0/\alpha_0=\{(\Delta^2+4T^2)^{1/2}-\Delta\}/2T. \tag{3}$$

When $\Delta>0$, as for example in NiO and CuO, $\beta_0/\alpha_0<1$ is obtained from Eq. (3). This implies that the $3d^n$ configuration ($n=8$, 9 for Ni(II) and Cu(II), respectively) dominates the ground state; in other words, the $3d^{n+1}\underline{L}$ contributions are small. It has been pointed out that Δ decreases by as much as 3 eV when going from Cu(II) to Cu(III), and can even become negative in materials like $NaCuO_2$ (Refs. 26 and 27) and $La_2Li_{0.5}Cu_{0.5}O_4$.[14] In this case, $\beta_0/\alpha_0>1$, which implies that the $3d^{n+1}\underline{L}$ configuration is the dominant one. The intensity of the pre-edge peak in the O-K XAS spectrum reflects then the fraction of holes residing in O $2p$ states, which is proportional to β_0^2.[14,23]

Problems can arise, however, in TM systems with higher oxidation states, where Δ remains positive. In such cases, the $3d^{n+1}\underline{L}$ configuration does not always dominate, and the result is a significant contribution from the $3d^n$ configuration to the ground state. An example for this behavior is the class of compounds $Ln_2Li_{0.5}TM_{0.5}O_4$, which formally contains TM(III) ions. In a previous study, a theoretical analysis of the TM-$L_{2,3}$ XAS spectra of these materials, with TM=Cu, Ni, and Co, has shown that the contribution of the $3d^n$ configuration to the ground state is as high as 30, 57, and 72%, respectively.[14] This highlights the problem discussed in the following. The observation of a doping-related increase in intensity of the pre-edge peak in the O-K XAS spectra for systems such as these can lead to oversimplified statements, such as ''the holes always go into the O $2p$ states.'' The validity of this statement depends critically on the details of the system involved, as can be seen from the $Ln_2Li_{0.5}TM_{0.5}O_4$ example discussed above.[14] Indeed, such considerations have led to the conclusion [28] that the ground state of $La_2Li_{0.5}Cu_{0.5}O_{4-\delta}$ contains *no* admixture of the $3d^8$ configuration at all, but can be written as $\alpha_0|3d^9\rangle+\beta_0|3d^9\underline{L}\rangle$. As mentioned above, a full analysis of the Cu-$L_{2,3}$ XAS data for this system gives a different picture, with a significant contribution (30%) of the $3d^8$ configuration to the ground state.[14]

The final state of a TM-$L_{2,3}$ XAS experiment can be described by a similar theoretical framework, where Δ in Eq. (1) is replaced by $U_f=\Delta-U_{cd}+U_{dd}$ (U_{cd} and U_{dd} represent the Coulomb interaction energies $2p/3d$ and $3d/3d$, respectively), and the other parameters have modified, ''final-state'' values.

It has been pointed out recently that the effects of covalency in XAS spectra can be enhanced by nonlocal effects.[29] As was briefly mentioned above, such nonlocal effects occur in systems where the TMO_6 octahedra form interconnected networks, leading, e.g., to a broadening of the spectral features, a shift to lower energies, and an increase in intensity of the pre-edge peak in case of the O-K XAS spectra. This is seen in Fig. 4 when going from the isolated cluster system $Nd_2Li_{0.5}Ni_{0.5}O_4$ to the Sr-doped system, which contains a continuous Ni-O network.

In order to arrive at a more quantitative understanding of the charge distribution in the two Ni(III) systems compared in Fig. 4, we present in the next section results of a calculation based on local NiO_6 clusters including charge-transfer, hopping, as well as a full multiplet interaction within a complete basis approach for these compounds.[15] We note that a complete-basis calculation expresses the ground-state wave function as

$$\Phi_g = \sum_i C_i |d^{n+i}\underline{L}^i\rangle, \tag{4}$$

where the summation over i is from 0 to $(10-n)$. This is in contrast to Eq. (2) where the summation over i corresponds to 0 and 1 only, with C_0 and C_1 being equal to α_0 and β_0.

C. Charge-transfer atomic-multiplet calculations

In these calculations, we have considered a single cluster with one Ni atom surrounded by six O atoms. In order to reduce the size of the Hamiltonian matrix without introducing any further approximation, only linear combinations of the O 2p orbitals with the same symmetry as the Ni 3d orbitals were considered. Apart from the O 2p and Ni 3d orbitals, the Ni 2p orbitals were also included in the calculations. The Hamiltonian used to describe the system includes the Coulomb interaction between the Ni 2p and 3d electrons, defined in terms of the Slater integrals F^0_{pd}, F^2_{pd}, G^1_{pd}, and G^3_{pd}, as well as that between the 3d electrons given by the Slater integrals F^0_{dd}, F^2_{dd}, and F^4_{dd}. The spin-orbit interaction has also been considered within the 2p and the 3d manifold at the transition-metal site, the strengths of which are determined by ξ_p and ξ_d, respectively. An ionic-crystal-field term was also included in the Hamiltonian to simulate the observed splitting of the fivefold degenerate d orbitals. While for the case of octahedral symmetry in $Nd_{0.9}Sr_{1.1}NiO_{3.95}$, the crystal-field splitting is expressed in terms of $10Dq$, for the D_{4h} symmetry in $Nd_2Li_{0.5}Ni_{0.5}O_4$, the splitting is defined by $10Dq$ and Ds. Hybridization has been included between the symmetry-adapted combinations of oxygen orbitals and Ni 3d orbitals. The charge transfer between the ligand and the transition-metal atom is determined by the ionic configuration at the transition-metal site and is defined as the difference between the multiplet-averaged energies of the d^n and $d^{n+1}\underline{L}$ configuration at the transition-metal atom:

$$\Delta = E^{\mathrm{av}}(d^{n+1}\underline{L}) - E^{\mathrm{ev}}(d^n) = e_d - e_p + n^*U. \tag{5}$$

Hence the charge-transfer energy can be expressed in terms of the bare energies of the 3d transition metal and the 2p ligand orbitals (e_d and e_p, respectively), the configuration n, and U, which is the multiplet-averaged Coulomb interaction strength between the 3d electrons. The multipole terms of the Coulomb interactions were set to 80% of the Hartree-Fock values, while the monopole terms, F^0_{dd} and F^0_{pd}, were estimated by fitting the experimental spectrum. The other parameters, $pd\sigma$, Δ, $10Dq$, and Ds, were estimated by fitting the experimental spectra. Although atomic values for the spin-orbit strength were usually seen to be sufficient, in some cases ξ_p was varied slightly to get a better fit of the experimental spectrum. For comparison with experiment, the spectral functions, evaluated by using the Lanczos method, were broadened by a Gaussian and an energy-dependent Lorentzian to simulate experimental resolution and lifetime effects, respectively.

TABLE I. Parameter set (in eV) used for the calculations as well as lthe resulting C_0^2 [which represents the $3d^n$ weight in the ground state: Eq. (4)] for NiO ($n=8$), $Nd_2Li_{0.5}Ni_{0.5}O_4$ ($n=7$), and $Nd_{0.9}Sr_{1.1}NiO_{3.95}$ ($n=7$).

	Δ	$pd\sigma$	$pd\pi$	U_{cd}	U_{dd}	C_0^2
$Nd_2Li_{0.5}Ni_{0.5}O_4$	1.5	−1.73	0.86	8.7	6.7	0.51
$Nd_{0.9}Sr_{0.1}NiO_{3.95}$	1.0	−2.0	1.0	8.0	6.7	0.42
NiO	4.0	−1.3	0.65	7.2	6	0.94

As a test case, we first treat the standard Ni(II) system NiO. The parameters obtained from a fit to the experimental spectra are given in Table I. For NiO, 94% $3d^8$ was obtained in the ground state, indicating a basically ionic Ni^{2+} state in agreement with the results of previous studies.[13]

As has been mentioned above, considering its slight oxygen deficiency, $Nd_{0.9}Sr_{1.1}NiO_{3.95}$ represents formally a pure Ni(III) state. The transition-metal site in both NiO and $Nd_{0.9}Sr_{1.1}NiO_{3.95}$ has the same octahedral symmetry. However, the structure in the Ni-L_3 XAS spectra at 854 eV is much weaker in NiO, whereas it is the most intense feature in the spectra of the two Ni(III) compounds. The results of a simulation of the spectra of all three Ni compounds are shown in the right panel of Fig. 4. With reference to Table I, it can be seen that, when moving from the Ni(II) to the Ni(III) compounds, the extracted parameters indicate an increase in covalency: the Ni(III) systems have larger hybridization strengths as well as reduced charge-transfer energies.

Comparing the two Ni(III) compounds, we can directly see the influence of nonlocal effects on the electronic configuration: $Nd_{0.9}Sr_{1.1}NiO_{3.95}$ is more covalent than $Nd_2Li_{0.5}Ni_{0.5}O_4$, which is a consequence of the continuous Ni-O network in the former material. To get a reasonable simulation of the experimental spectra, we have to increase Δ and decrease $pd\sigma$ from $Nd_{0.9}Sr_{1.1}NiO_{3.95}$ to $Nd_2Li_{0.5}Ni_{0.5}O_4$. This means that the $3d^7$ contribution in the ground state in the former material is 42% as compared to 51% in the isolated cluster system. Nevertheless, these data and their theoretical analysis clearly show that the general trend derived from the lithium-doped system is preserved: the doping-induced holes have a substantial Ni 3d weight in systems with a formal Ni(III) oxidation state.

IV. CONCLUSIONS

We have presented the results of an experimental study of both the O-K and Ni-$L_{2,3}$ XAS spectra of the nickelate

$Nd_{2-x}Sr_xNiO_{4-\delta}$, together with a detailed theoretical analysis of the Ni-$L_{2,3}$ XAS spectra within a charge-transfer atomic-multiplet approach. The experimental spectra represent a reliable data recorded at the Ni-$L_{2,3}$ thresholds for this system, as the choice of Nd avoids overlap of the La-M_4 with the Ni-L_3 XAS spectra, which has marred experiments on the La analog up till now. The main points arising from the experimental spectra and their theoretical interpretation are as follows:

• The number of hole states in the O $2p$ orbitals increases linearly with the doping level x up to the maximum value studied of $x=1.4$. Previous reports of a saturation of the O-K pre-edge spectral weight for high x values are not confirmed and are probably due to surface oxygen deficiency.

• The holes induced by Sr doping reside, about equally, in the Ni $3d$ and O $2p$ orbitals. This is expressed in terms of a ground-state population of 42% for the $3d^7$ configuration in the formal Ni(III) system $Nd_{0.9}Sr_{1.1}NiO_{3.95}$.

• Comparison of the experimental and theoretical results for the two pure Ni(III) systems, $Nd_{0.9}Sr_{1.1}NiO_{3.95}$ and $Nd_2Li_{0.5}Ni_{0.5}O_4$, shows that the nature of the Ni-O network has a significant influence on the degree of covalency in these systems. Specifically, the inter-NiO_6-cluster interaction in the Sr-doped system enhances covalency with respect to that in the isolated NiO_6-cluster system $Nd_2Li_{0.5}Ni_{0.5}NiO_4$.

ACKNOWLEDGMENTS

This work was supported by the Deutsche Forschungsgemeinschaft, Project Nos. Fi439/7-1 and Ka564/7-1. Z.H. thanks the Graduiertenkolleg ''Struktur-und Korrelationseffekte im Festkörper'' at the Technical University Dresden for financial support. We are grateful to Professor G. van der Laan for valuable discussions.

[1] G. Aeppli and D. J. Buttrey, Phys. Rev. Lett. **61**, 203 (1988).
[2] J. D. Jorgensen, B. Dabrowski, S. Pei, D. R. Richards, and D. G. Hinks, Phys. Rev. B **40**, 2187 (1990).
[3] R. J. Cava, B. Batlogg, T. T. M. Palstra, J. J. Krajewski, W. F. Peck, Jr., A. P. Ramirez, and L. W. Rupp, Jr., Phys. Rev. B **43**, 1229 (1991).
[4] Priya Mahadevan, K. Sheshadri, D. D. Sarma, H. R. Krishnamurthy, and Rahul Pandit, Phys. Rev. B **55**, 9203 (1997).
[5] P. Ganguly and C. N. R. Rao, J. Solid State Chem. **53**, 193 (1984).
[6] K. Sreedhar and C. N. R. Rao, Mater. Res. Bull. **25**, 1235 (1990).
[7] E. Pellegrin, J. Zaanen, H.-J. Lin, G. Meigs, C. T. Chen, G. H. Ho, H. Eisaki, and S. Uchida, Phys. Rev. B **53**, 10 667 (1996).
[8] P. Kuiper, J. van Elp, G. A. Sawatzky, A. Fujimori, S. Hosoya, and D. M. de Leeuw, Phys. Rev. B **44**, 4570 (1991).
[9] C. H. Chen, S.-W. Cheong and A. S. Cooper, Phys. Rev. Lett. **71**, 2461 (1993).
[10] H. Eisaki, S. Uchida, T. Mizokawa, H. Namatame, A. Fujimori, J. van Elp, P. Kuiper, G. A. Sawatzky, S. Hosoya, and H. Katayama-Yoshida, Phys. Rev. B **45**, 12 513 (1992).
[11] P. Kuiper, D. E. Rice, D. J. Buttrey, H.-J. Lin, and C. T. Chen, Physica B **208**, 271 (1995).
[12] See, e.g., J. Fink, N. Nücker, E. Pellegrin, H. Romberg, M. Alexander, and M. Knupfer, J. Electron Spectrosc. Relat. Phenom. **66**, 395 (1994).
[13] F. M. F. de Groot, J. C. Fuggle, B. T. Thole, and G. A. Sawatzky, Phys. Rev. B **42**, 5459 (1989).
[14] Z. Hu, C. Mazumdar, G. Kaindl, F. M. F. de Groot, S. A. Warda, and D. Reinen, Chem. Phys. Lett. **297**, 321 (1998).
[15] Priya Mahadevan and D. D. Sarma (unpublished).
[16] D. Reinen, U. Kesper, and D. Belder, J. Solid State Chem. **116**, 355 (1995).
[17] L. Tröger, D. Arvanitis, K. Baberschke, H. Michaelis, U. Grimm, and E. Zschech, Phys. Rev. B **46**, 3283 (1992).
[18] J. Jaklevic, J. A. Kirby, M. P. Klein, and A. S. Robertson, Solid State Commun. **23**, 679 (1997).
[19] H. Eskes, M. B. J. Meinders, and G. A. Sawatzky, Phys. Rev. Lett. **67**, 1035 (1991).
[20] S. M. Butorin, J.-H. Guo, L.-C. Duda, N. Wassdahl, J. Nordgren, E. Z. Kurmaev, and S. P. Tolochko, Physica C **235-240**, 1047 (1994).
[21] M. Medarde, A. Fontaine, J. L. García-Muñoz, J. Rodríguez-Carvajal, M. de Santis, M. Saccchi, G. Rossi, and P. Lacorre, Phys. Rev. B **46**, 14 975 (1992).
[22] S. A. Warda, W. Pietzuch, G. Beighöfer, U. Kesper, W. Massa, and D. Reinen, J. Solid State Chem. **138**, 18 (1998).
[23] P. Kuiper, G. Kruizinga, J. Ghijsen, G. A. Sawatzky, and H. Verweij, Phys. Rev. Lett. **62**, 221 (1989).
[24] P. Kuiper, J. van Elp, D. E. Rice, D. J. Buttrey, H.-J. Lin, and C. T. Chen, Phys. Rev. B **57**, 1552 (1998).
[25] V. I. Anisimov, S. Yu. Ezhov, and T. M. Rice, Phys. Rev. B **55**, 12 829 (1997).
[26] D. D. Sarma, C. T. Simmons, O. Strebel, U. Neukirch, G. Kaindl, R. Hoppe, and H. P. Muller, Phys. Rev. B **37**, 9784 (1988); Seva Nimkar, D. D. Sarma, and H. R. Krishnamurthy, *ibid.* **47**, 10 927 (1993); Seva Nimkar, N. Shanthi, and D. D. Sarma, Proc.-Indian Acad. Sci., Chem. Sci. **106**, 393 (1994).
[27] T. Mizokawa, H. Namatame, K. Fujimori, H. Akeyama, H. Kondoh, H. Kurada, and Kosugi, Phys. Rev. Lett. **67**, 1638 (1991).
[28] N. Merrien, F. Studer, C. Michel, P. Srivastava, B. R. Sekhar, N. L. Saini, K. B. Garg, and G. Tourillon, J. Phys. Chem. Solids **54**, 499 (1993).
[29] K. Okada and A. Kotani, J. Electron Spectrosc. Relat. Phenom. **88-91**, 255 (1998).